

Daniel J.V.A. dos Santos  
José A.N.F. Gomes

## Chain length effect on the structure of alkyltrimethylammonium chloride monolayers between two immiscible liquids

**Abstract** The main purpose of this article is to understand at the microscopic level the possible effect of the chain length on the properties of an adsorbed monolayer between two immiscible liquids. We report a molecular dynamics simulation study of an alkyltrimethylammonium chloride monolayer adsorbed in the water/isooctane interface. The surfactants studied have 8, 12 and 16 carbon atoms in the chain and are studied at a constant area of  $45 \text{ \AA}^2$  per surfactant. It was found that the chain widths of the number density profile distributions increase with the chain length and the tilt angle distribution does not change with the chain length. There is also no correlation between the percentage of trans conformations in an alkyltrimethylammonium chain and

the length of the chain. The probability of finding a given number of trans conformations per chain is also similar in the three different surfactants. An increase of four methylene groups in the central part of the chain just displaces this distribution by about two trans conformations. The mean-square displacement of the terminal methyl group of the alkyltrimethylammonium chains is also very similar in the different surfactant types. Our results support the conclusions of Bell et al. [(1998) *J. Phys. Chem. B* 102:218] concerning the structures of the alkyltrimethylammonium monolayers (they are very similar and independent of the chain length).

**Keywords** Self-assembly · Monolayers · Molecular dynamics

D.J.V.A. dos Santos (✉)  
José A.N.F. Gomes  
CEQUP/Departamento de Química da  
Faculdade de Ciências da Universidade  
do Porto, R. Campo, Alegre 687,  
4069-007 Porto, Portugal  
e-mail: dasantos@fc.up.pt

### Introduction

Molecular monolayers and thin films have been extensively studied and play an important economic and scientific role. They are used extensively, for example, in the mining and oil industry for extraction and separation, or in the household industry for fabric softeners [1]. Clear evidence of the extensive experimental work in this field of chemistry is the appearance in the literature of several reviews [1, 2, 3, 4, 5, 6].

The knowledge of the relationship between the surfactant molecular structure and the macromolecular interfacial structure is important to understand and predict the performance of the surfactant. Yet, only

recently the molecular behaviour of the monolayers could be obtained thanks to the advent of new experimental techniques, like vibrational sum-frequency-generation spectroscopy [7, 8], neutron reflection [9, 10, 11, 12, 13, 14], or scanning tunnelling microscopy [15, 16], that can provide information on interfacial phenomena at a molecular level. With this new information, the data obtained by computer simulation can now be more thoroughly compared and validated.

Extensive theoretical [17, 18, 19] and experimental work (see the reviews already cited and the references therein) has been performed for Langmuir and Langmuir–Blodgett interfaces but only recently a small number of simulation studies have been performed on

monolayers between two immiscible liquids [20, 21, 22, 23].

Monolayers between two immiscible liquids are suitable for studies by electrochemistry techniques, namely cyclic voltammetry. They are easily built, mechanically stable, and the potential drop across the interface can be accurately controlled externally [24, 25, 26, 27]. The molecular behaviour of a monolayer between two immiscible liquids is very difficult to study even by the newest experimental techniques. Nevertheless, Conboy et al. [28] have applied vibrational sum-frequency spectroscopy to a series of monolayers adsorbed at the deuterated water and carbon tetrachloride interface and Lu and coworkers [29, 30] have studied a monolayer of monododecyl pentaethylene glycol at the solution/air interface with and without an oil layer of dodecane and dodecyltrimethylammonium ( $C_{12}TA$ ) bromide and hexadecyltrimethylammonium ( $C_{16}TA$ ) bromide monolayers mixed with dodecane at the water/air interface by neutron reflectometry.

Lyttle et al. [31] have studied by neutron reflection a series of alkyltrimethylammonium ( $C_nTA$ ) bromide monolayers with different chain lengths. They found that the monolayer thickness is constant and independent of the length of the carbon chain. For this to occur, the density of the monolayer and the mean tilt of the surfactant chains must increase as the chain length increases. On the other hand, Bell et al. [7] studied this same series of monolayers by sum-frequency spectroscopy and ellipsometry and found that neither the mean chain tilt nor the density varies significantly with the chain length.

Molecular dynamics can provide insightful information and help to clarify this issues. On the other hand, there is some information at the molecular level that despite the advances in the experimental techniques is still not yet accessible, but can be obtained by this type of computer simulation.

## Simulation details

For the water potential we used the simple point-charge model [32]. For the  $C_{16}TA$  we used the charges calculated by Böcker et al. [33] with the van der Waals and ligand forces parameterisation of the CHARMM22 [34] force field except for the dihedral angle, which was replaced by the Ryckaert-Bellemans [35, 36] description.

To obtain the charges for the other  $C_nTA$  ions,  $C_8TA$  and  $C_{12}TA$ , the Gaussian98 [37] ab initio computer program was used with the 6-31G\* basis set in a way similar to that used by Böcker et al. [33]. The charges on the sites of the united atom model were obtained by a Mulliken population analysis and they were found to be independent of the surfactant carbon tail length.

For isooctane (ISO) we used the same parameters as for the  $C_nTA$  carbon chains with no partial charges. For the chloride ion we used the parameters developed by Smith and Dang [38]. The water angle and all bond lengths were constrained using the SHAKE [39] algorithm with a tolerance of  $10^{-5}$  Å. To obtain

the Lennard-Jones parameters between sites of unlike atoms the Lorentz-Berthelot [34, 40] mixing rule was used (as required by the CHARMM22 potential).

All simulations were performed with a modified version of the DL\_POLY [41] molecular dynamics package in the *NAT* ensemble (300 K and an area of  $45 \text{ \AA}^2$  per head group) using a Nosé-Hoover [42, 43] thermostat in the implementation of Melchionna et al. [44].

Periodic boundary conditions were applied in the monolayer surface ( $x$ - and  $y$ -axes) but not for the longitudinal axis, in which the system interfaces with vacuum. In all simulations the velocity Verlet algorithm was used for the integration of the equations of motion with a time step of 2 fs. A  $10\text{-\AA}$  cutoff was used for the short-range interactions and a  $12\text{-\AA}$  one for the long-range interactions, with a smoothing function [45] applied between 11 and 12 Å. A multiple time step was also used for interactions greater than  $11.5 \text{ \AA}$  with an update frequency of eight time steps. A system check in the microcanonical ensemble was performed to verify the validity of the parameters and good energy conservation was found.

The system was prepared by constructing a square lattice monolayer with 100  $C_{16}TA$  ions with  $45 \text{ \AA}$  per head group. This corresponds to a cross-section of about  $67 \times 67 \text{ \AA}^2$ . All the dihedral angles of the  $C_{16}TA$  tails were set in a trans conformation and parallel to the  $z$ -axis. Chloride ions were added at a distance of about  $3\text{--}4 \text{ \AA}$  from the  $C_{16}TA$  head positions. A rapid equilibration was performed with the positions of the nitrogen atoms frozen while the tails were randomised – changing the orientation and the dihedral conformations. In all the following simulations the nitrogen atom positions were free to move according to Newtonian dynamics.

A water box with 4,500 molecules and a box containing 753 isooctane molecules, with the same cross-section of about  $50 \times 50 \text{ \AA}^2$ , were equilibrated for 150 ps in the *NpT* ensemble with periodic boundary conditions and simulation parameters similar to those described for the  $C_{16}TA$  chloride lattice.

The water molecules split across the boundaries were reunited and a system corresponding to a Langmuir interface was constructed by joining together the  $C_{16}TA$  chloride layer and the water box with a gap of  $3\text{--}4 \text{ \AA}$  between them. A new equilibration of 300 ps was performed in the *NAT* ensemble with periodic boundary conditions in all axes except the longitudinal  $z$ -axis. The molecules of the isooctane box which were split across the boundaries were also joined together. Finally, the monolayer between water/isooctane was constructed by joining the oil box to the Langmuir interface using a gap of  $3\text{--}4 \text{ \AA}$  between the  $C_{16}TA$  tails and the oil molecules. This system has a length of about  $100 \text{ \AA}$  along the major  $z$ -axis. The molecules interface with a vacuum at both ends of the longitudinal  $z$ -axis and have periodic boundary conditions in the monolayer plane ( $x$ -axis and  $y$ -axis).

This system was equilibrated for, at least, 1,200 ps. The other two monolayer systems with surfactants containing eight and 12 carbon atoms were constructed by subtracting from the first equilibrated system the excess carbon atoms in the surfactant tails. Both systems were equilibrated for at least 700 ps. In this way we obtained three systems with monolayers adsorbed between water and isooctane that only differ in the number of atoms in the carbon chains (8, 12 and 16).

After this equilibration, a production run of 1,000 ps on the three systems was started. During this production run the trajectories of the particles present in the systems were written to three different files every 32 steps and were analysed later.

## Results

The simulated system containing the  $C_{16}TA$  monolayer is represented by the average density profile in Fig. 1. The

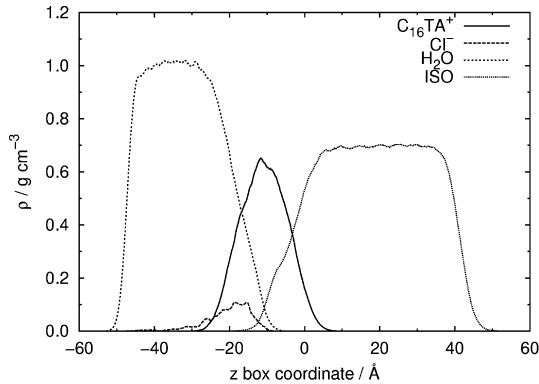


**Fig. 1** Average density profiles for the water, chloride ions isooctane and hexadecyltrimethylammonium ( $C_{16}TA$ ) ions as a function of the box coordinate

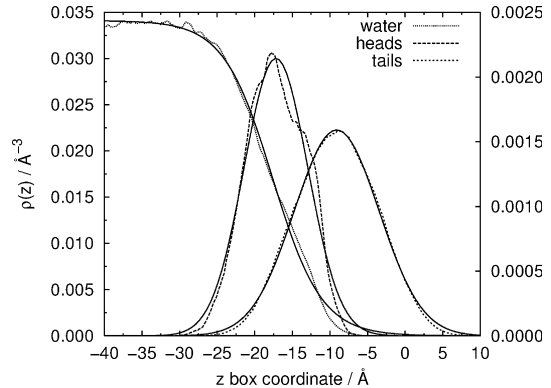


**Fig. 2** Profiles for the water and  $C_{16}TA$  (heads and tails) number densities at the water/isooctane interface. The fits are also displayed. The water scale is on the left-hand side

other two systems are also very similar and for all we could see the density profiles match the bulk densities of the liquids (water 0.997 and isooctane 0.6980 g cm<sup>-3</sup>) [46].

The simulation with the  $C_8TA$  monolayer is intended to test our results a step further since the carbon tail is very short. We performed a similar simulation with the  $C_8TA$  surfactant adsorbed at the water/2-heptanone interface and found that the monolayer was not stable. In the physically short simulation time, the surfactant started to dissolve into the 2-heptanone lamellae and also started to form a double layer. The stability of this monolayer when adsorbed in the water/isooctane interface is due to the fact that isooctane is much more hydrophobic than 2-heptanone. The water solubility in 2-heptanone is rather high, for an oil.

In the density profile for the three systems we could see a diffuse electrical double layer formed by a negatively charged diffuse barrier of chloride ions and a positively charged diffuse barrier of  $C_nTA$  heads ( $n=8, 12$  and  $16$ ). The penetration of the water molecules stops at the point where there are no more heads to be solvated. The diffuse layer of chloride ions is located mainly near the  $C_nTA$  heads, but some of the ions diffuse throughout the water slab.

The number density profiles were calculated for the water and  $C_nTA$  heads and tails, for the three different surfactants. As an example, in Fig. 2 we present  $C_{16}TA$

and water number density profiles. The fits to the water profiles were done using the same hyperbolic tangent function that is commonly used to fit experimental data [6]:

$$\rho = \frac{\rho_0}{2} \left[ 1 \pm \tanh \left( \frac{z - z_0}{\zeta} \right) \right] \quad (1)$$

where  $\zeta$  is the width of the distribution and  $z_0$  is the centre.

For the  $C_nTA$  heads and tails, a Gaussian function was used:

$$\rho = \rho_0 \exp \left[ -4 \left( \frac{(z - z_0)^2}{\sigma^2} \right) \right], \quad (2)$$

where  $\sigma$  is the width of the distribution and  $z_0$  is also the centre. The parameters obtained by fitting the simulation results are presented in Table 1.

Although the experimental results presented in Table 1 were obtained for a series of  $C_nTA$  monolayers where the counterion was bromide and not chloride, and at the water/air interface instead of the water/isooctane interface, the fitting parameters agree quite well. Aromatic anions can cause a major change in the structure of monolayers [8], but in our case, since the nature of the counterions is similar, this effect is absent and the experimental and simulation results can be directly

**Table 1** Widths  $\zeta$  and  $\sigma$  of the water and alkyltrimethylammonium ( $C_nTA$ ) head and tail profiles as defined by Eqs. (1) and (2).  $\delta_{ij}$  are the separations between the distribution centres (chains,  $c$ , heads,  $h$ , water,  $s$ ). The experimental values were taken from Refs. [6, 31]

Surfactant	$\sigma_h/\text{\AA}$	$\sigma_c/\text{\AA}$	$\zeta/\text{\AA}$	$\delta_{ch}/\text{\AA}$	$\delta_{hs}/\text{\AA}$	$\delta_{cs}/\text{\AA}$
$C_8TA$ – this work	$11.80 \pm 0.09$	$11.67 \pm 0.03$	$6.45 \pm 0.06$	$4.90 \pm 0.04$	$0.22 \pm 0.07$	$5.12 \pm 0.05$
$C_{12}TA$ – this work	$12.0 \pm 0.1$	$13.42 \pm 0.03$	$6.59 \pm 0.07$	$6.70 \pm 0.05$	$0.22 \pm 0.08$	$6.93 \pm 0.05$
$C_{12}TA$ – exp	$12.5 \pm 3$	$16.0 \pm 1$	$5.5 \pm 0.5$	$6.5 \pm 1$	$1 \pm 1$	$7.0 \pm 1$
$C_{16}TA$ – this work	$12.0 \pm 0.1$	$15.96 \pm 0.04$	$6.50 \pm 0.06$	$8.07 \pm 0.05$	$0.44 \pm 0.07$	$8.51 \pm 0.05$
$C_{16}TA$ – exp	$14 \pm 3$	$16.5 \pm 1$	$6.5 \pm 1$	$8.5 \pm 1$	$2 \pm 1.5$	$9.0 \pm 1$

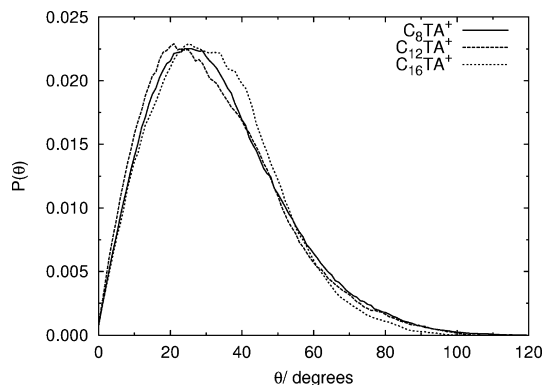


**Fig. 3** Tilt angle distributions for the alkyltrimethylammonium ( $C_nTA$ ) ions adsorbed at the water/ISO interface

compared. The presence of the isooctane oil layer instead of air can change some properties, namely the average mean tilt angle (Eq. 3). The tilt angle distribution can be different if a monolayer is adsorbed at the water/air instead of at the water/oil interface, but cannot modify a consistent change in behaviour with the chain length at the same interface.

The major difference between the fitting parameters obtained by simulation and those obtained by neutron reflection refer to the values for  $\sigma$  of the chains. The experimental values for  $\sigma_c$  let Penfold and coworkers state that the thickness of the monolayer is independent of the chain length (about 16 Å for the surfactant series). On the other hand, our results agree with the conclusion of Bell et al. [7] since there is an increase in the width of the chain distribution profile as the chain length increases.

The tilt angle,  $\theta$ , is defined as

$$\theta = \arccos\left(\mathbf{Z} \cdot \frac{\mathbf{R}_{1N}}{|\mathbf{R}_{1N}|}\right), \quad (3)$$

where  $\mathbf{R}_{1N}$  is the vector between the nitrogen atom and the terminal methyl group in the same molecule,  $\mathbf{R}_1 - \mathbf{R}_N$ , and  $\mathbf{Z}$  is the unit vector of the  $z$ -axis. This angle was calculated over all the  $C_nTA$  ions and a probability distribution was obtained for each surfactant type.

As can be seen in Fig. 3 the tilt angle distribution does not change when changing the chain length. For the three distributions, the maximum probability is located between 20 and 30° and the average angle is about  $33 \pm 18^\circ$ . We can conclude that for a surfactant monolayer at the same coverage density, the tilt angle distribution and consequently the mean tilt do not change when the length of the chain changes. Bell et al. also found that neither the density nor the mean tilt angle varies significantly with the chain length.

The percentage of trans conformations as a function of the dihedral number in the chains of the  $C_nTA$  series is presented in Fig. 4. Similar behaviour occurs for this

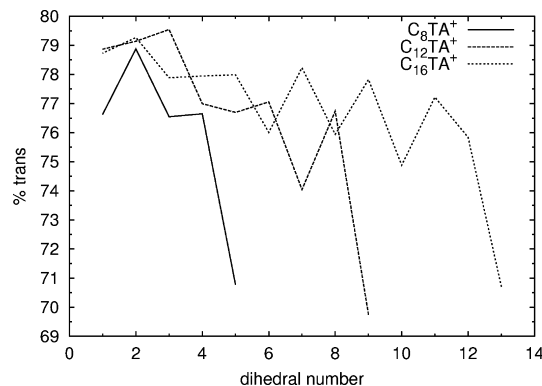


**Fig. 4** Percentage of trans conformations in the  $C_nTA$  hydrocarbon chains as a function of the dihedral number. On the left-hand side we found the water lamellae and on the right-hand side the ISO lamellae

$C_nTA$  series: when one goes through the  $C_nTA$  chain from the water into the oil phase, the number of trans conformations decreases and the terminal dihedral has the greater percentage of gauche conformations. The percentage of trans conformations for the terminal dihedral of the chain is almost the same for the three different surfactants. This also occurs with the penultimate and with the dihedral angles that are closer to the surfactant heads. This behaviour means that when we increase the chain length by introducing methylene groups in the middle of the chain, the average conformation remains unchanged and we are just introducing dihedral angles with similar conformations in the central part of the chain. This also agrees with the findings of Bell et al. [7].

The independence of the conformation of the chains upon the chain length is also clearly seen when we calculate the probability of finding a given number of trans conformations per chain and discover that they are similar (Fig. 5). An increase of four methylene groups in the central part of the chain just displaces this distribution by about two trans conformations.

Several order parameters can be obtained by the following tensor [47]:

$$S_{ij} = 1/2\langle 3 \cos \theta_i \cos \theta_j - \delta_{ij} \rangle, \quad (4)$$

where  $\theta_i$  is the angle between the  $i$ th molecular axis and the monolayer normal –  $z$ -axis. The order parameter is a measure of the deviation from the monolayer normal. For each  $CH_2$  unit we can define the  $z$ -axis as the vector from the  $C_{n-1}$  to the  $C_{n+1}$  unit; the  $y$ -axis is the vector in the plane of these two units and is perpendicular to the  $z$ -axis; the  $x$ -axis is perpendicular to the  $y$ -axis and the  $z$ -axis.

The chain order parameter is usually defined as

$$S_{zz} = 1/2\langle 3 \cos \theta_i \cos \theta_j - 1 \rangle \quad (5)$$

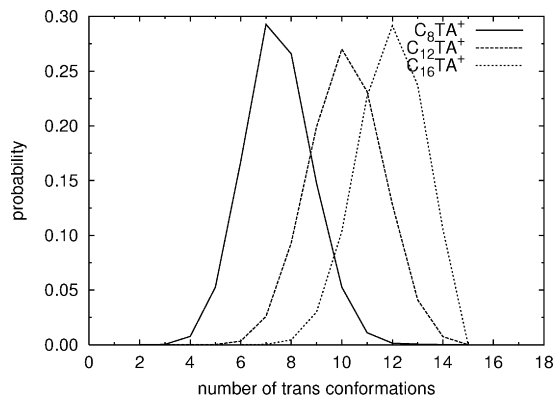


**Fig. 5** Probability of finding a given number of trans conformations for each  $C_n$ TA surfactant type

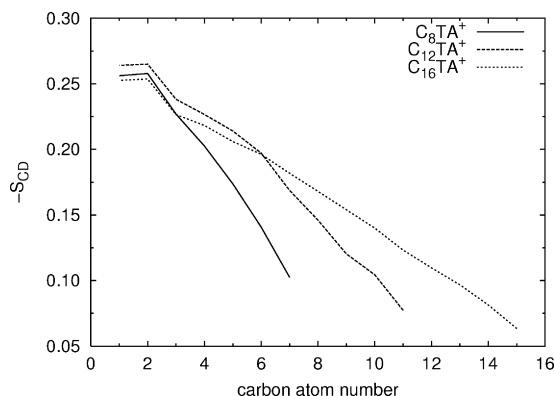


**Fig. 6** Average deuterium order parameter as a function of methyl carbon atom number for each  $C_n$ TA surfactant type. The water slab is located on the left-hand side and the oil slab on the right-hand side

and is related to the local order of the long molecular axis. The experimentally observed deuterium NMR order parameter can be obtained using Eq. (6):

$$S_{CD} = 2/3S_{xx} + 1/3S_{yy}. \quad (6)$$

The values for the chain order parameter and for the deuterium order parameter (Fig. 6) were calculated and found to be in good agreement with the experimental values for other surfactant types [22, 23, 48].

For all three different surfactants, the randomness in the orientation increases from the head to the tail and similar behaviour as described for the percentage of trans conformations in the  $C_n$ TA hydrocarbon chains occurs. The addition of methylene groups modifies the slope of the curve but maintains the same characteristics: the order parameters for the carbon atoms near the heads and at the end of the tails remain the same, the only difference remains at the central part of the chains.

The bond order parameter was calculated using the bond vector as the molecular axis and is a measure of the average inclination of the bond axes with respect to

the monolayer normal. The differences between the three surfactant types and the evolution of the bond order parameter as one goes from the head to the tail of a given surfactant type is similar to the description already made for the other order parameters. However, the seesaw-like behaviour is more pronounced for the surfactants with the longest chains.

The in-plane mean-square displacement for the terminal methyl group of the  $C_n$ TA chains was calculated and was found to be very similar between the different surfactant types, but a positive correlation exists with the chain length. This was to be expected since for the longer chains a trans-to-cis conformation conversion in the central part of the chain makes a large movement of the terminal methyl group.

We can use the Einstein relation [40] for two dimensions and valid for long times to calculate the diffusion coefficient parallel to the interface:

$$D = \lim_{t \rightarrow \infty} \frac{1}{4t} \langle |r_i(t) - r_i(0)|^2 \rangle, \quad (7)$$

where  $r_i(t)$  is the particle position at time  $t$ . Using this relation to calculate the diffusion constant,  $D$ , for the terminal methyl group, we find values of  $6.80 \times 10^{-6}$ ,  $5.99 \times 10^{-6}$  and  $5.59 \times 10^{-6}$   $\text{cm}^2 \text{s}^{-1}$ , for  $C_{16}$ TA,  $C_{12}$ TA and  $C_8$ TA, respectively. These values are in fair agreement with those obtained by Tarek et al. [49] for the lateral diffusion of the tetradecyltrimethylammonium mass centre.

## Summary and conclusions

In the present study we reported on a molecular dynamics simulation study of a  $C_n$ TA chloride monolayer (with  $n=8, 12$  and  $16$ ) between the water/isooctane interface. Both the collective and the individual properties of the  $C_n$ TA ions were studied and a comparison was made in order to try to understand the influence of the chain length on the static and dynamic microscopic properties of the monolayer. Our results are in good agreement with available experimental and simulation data.

A diffuse electrical double layer was found, formed on one side by a diffuse negative layer of chloride ions and on the other by a diffuse positively charged layer formed by the  $C_n$ TA heads.

When analysing the number density profile distributions, we could find that when varying the surfactant chain length the head-group widths remain unchanged; however, the chain widths increase with the chain length. The tilt angle distribution does not change with the chain length; the maximum probability is located between 20 and 30° and the average angle is about  $33 \pm 18^\circ$ .

The average number of trans conformations per chain exhibits similar behaviour for this  $C_n$ TA series. When the

chain length increases, the average number of trans conformations remains unchanged and we are just introducing dihedral angles with similar conformations in the central part of the chain. The probability of finding a given number of trans conformations per chain is also similar in the three different surfactants. An increase of four methylene groups in the central part of the chain just displaces this distribution by about two trans conformations.

The mean-square displacement of the terminal methyl group of the  $C_nTA$  chains is very similar among the different surfactant types. Nevertheless, when the chain length increases, the diffusion coefficient also increases because a trans-to-cis conformation conversion in the central part of the chain leads to a large movement of the terminal methyl group.

The data that best characterise the monolayer and surfactant behaviour, namely the width of the number density profiles for the chains, the distance between the distribution centres of the heads and tails, the tilt angle distribution and the percentage of trans conformations, lead us to suggest, in harmony with the findings of Bell et al. [7], that the structures of the  $C_nTA$  monolayer studied are very similar and are independent of the chain length.

**Acknowledgements** D.J.V.A.d.S. thanks the Programa PRAXIS XXI for a doctoral scholarship (BD/15576/98). It is also a pleasure to thank Natália Cordeiro for stimulating discussions. Finally, I am deeply indebted to Elsa Henriques for the manipulation of the Quanta computer program.

## References

- Swalen JD, Allara DL, Andrade JD, Chandross EA, Garoff S, Israelachvili J, McCarthy TJ, Murray R, Pease RF, Rabolt JF, Wynne KJ, Yu H (1987) *Langmuir* 3:932
- Shinoda K, Lindman B (1987) *Langmuir* 3:135
- Whitesides GM, Laibinis P (1990) *Langmuir* 6:87
- Gelbart WM, Ben-Shaul A (1996) *J Phys Chem* 100:13169
- Miranda PB, Shen YR (1999) *J Phys Chem B* 103:3292
- Lu JR, Thomas RK, Penfold J (2000) *Adv Colloid Interface Sci* 84:143
- Bell GR, Manning-Benson S, Bain CD (1998) *J Phys Chem B* 102:218
- Bell GR, Bain CD, Li ZX, Thomas RK, Duffy DC, Penfold J (1997) *J Am Chem Soc* 119:10227
- Simister EA, Lee EM, Thomas RK, Penfold J (1992) *J Phys Chem* 96:1373.
- Lu JR, Hromadova M, Simister BA, Thomas RK, Penfold J (1994) *J Phys Chem* 98:11519
- Lu JR, Li ZX, Smallwood J, Thomas RK, Penfold J (1995) *J Phys Chem* 99:8233
- Lu JR, Li ZX, Thomas RK, Penfold J (1996) *J Chem Soc Faraday Trans* 92:403
- Lu JR, Thomas RK (1998) *J Chem Soc Faraday Trans* 94:995
- Penfold J (2002) *Curr Opin Colloid Interface Sci* 7:139
- Wu P, Zeng Q, Xu S, Wang C, Yin S, Bai C-L (2002) *CHEMPHYSICHEM* 2:750
- Xu S-L, Wang C, Zeng Q-D, Wu P, Wang Z-G, Yan H-K, Bai C-L (2002) *Langmuir* 18:657
- da Gama MMT, Gubbins KE (1986) *Mol Phys* 59:227
- Vincze A, Horvai G, Leermakers FAM (1995) *Electrochim Acta* 40:2875
- Rieu JP, Vallade M (1996) *J Chem Phys* 104:729
- Schweighofer K, Essmann U, Berkowitz M (1997) *J Phys Chem B* 101:3793
- Schweighofer K, Essmann U, Berkowitz M (1997) *J Phys Chem B* 101:10775
- Dominguez H, Smondyrev AM, Berkowitz ML (1999) *J Phys Chem B* 103:9582.
- Dominguez H, Berkowitz ML (2000) *J Phys Chem B* 104:5302
- Wandlowski T, Marecek V, Samec Z (1988) *J Electroanal Chem* 242:277
- Kakiuchi T, Nakanishi M, Senda M (1989) *Bull Chem Soc Jpn* 62:403
- Kakiuchi T, Kondo T, Kotani M, Senda M (1992) *Langmuir* 8:169
- Cunnane VJ, Schiffrin DJ, Fleischmann M, Geblewicz G, Williams D (1988) *J Electroanal Chem* 243:455
- Conboy JC, Messner MC, Richmond GL (1997) *J Phys Chem* 101:6724
- Lu JR, Thomas KK, Binks BP, Fletcher PDI, Penfold J (1995) *J Phys Chem* 99:4113
- Lu JR, Li ZX, Thomas RK, Binks BP, Crichton P, Fletcher PDI, McNab JR, Penfold J (1998) *J Phys Chem B* 102:5785
- Lyttle PJ, Lu JR, Su TJ, Thomas RK, Penfold J (1995) *Langmuir* 11:1001
- Berendsen HJ, Postma JPM, van Gunsteren WF, Hermans J (1981) In: Pullman B (ed) *Intermolecular forces*. Reidel: Dordrecht, pp 33
- Böcker J, Schlenkrich M, Bopp P, Brickmann J (1992) *J Phys Chem* 96:9915
- MacKerell RAD Jr et al (1998) *J Phys Chem B* 102:3586
- Ryckaert J-P, Bellemans A (1975) *Chem Phys Lett* 30:123
- Ryckaert J-P, Bellemans A (1978) *Faraday Discuss Chem Soc* 66:95
- Frisch MJ et al (2001) *Gaussian 98*, revision A.11.2. Gaussian, Pittsburgh, PA
- Smith PB, Dang LX (1994) *J Chem Phys* 100:3757
- Ryckaert J-P, Ciccotti C, Berendsen HJC (1977) *J Comput Phys* 23:327
- Allen MP, Tildesley DJ (1990) *Computer simulation of liquids*. Oxford University Press, Oxford
- Forrester PW, Smith W (1998) *DL\_POLY*, version 2.11. CCLRC Daresbury Laboratory, Daresbury, UK
- Nosé S (1991) In: Meyer M, Pontikis V (eds) *Computer simulation in materials science*. Kluwer, Dordrecht, pp 21
- Hoover WG (1985) *Phys Rev A* 31:1695
- Melchionna S, Ciccotti G, Holian BL (1993) *Mol Phys* 78:533
- Brooks CL III, Pettitt BM, Karplus M (1985) *J Chem Phys* 83:5897
- Weast RC (1990) *Handbook of chemistry and physics*. CRC, Boca Raton, FL
- Egberts B, Berendsen HJC (1988) *J Chem Phys* 89:3718
- Sheng Q, Shulten K, Pidgeon C (1995) *J Phys Chem* 99:11018
- Tarek M, Tobias DJ, Klein ML (1995) *J Phys Chem* 99:1393